Journal of Organometallic Chemistry 890 (2019) 13–20

Contents lists available at ScienceDirect

Journal of Organometallic Chemistry

journal homepage: www.elsevier.com/locate/jorganchem

Synthesis, characterization and single crystal X-ray studies of pincer type Ni(II)-Schiff base complexes: Application in synthesis of 2-substituted benzimidazoles

Bhumika Agrahari [a], Samaresh Layek [a], Rakesh Ganguly [b], Necmi Dege [c], Devendra D. Pathak [a, *]

[a] Department of Applied Chemistry, Indian Institute of Technology (Indian School of Mines), Dhanbad, 826004, India
[b] Division of Chemistry & Biological Chemistry, Nanyang Technological University, Singapore, 639798, Singapore
[c] Ondokuz Mayıs University, Arts and Sciences Faculty, Department of Physics, 55139, Samsun, Turkey

ARTICLE INFO

Article history:
Received 18 February 2019
Received in revised form
19 March 2019
Accepted 22 March 2019
Available online 27 March 2019

Keywords:
Pincer type
Nickel
Crystal structure
Benzimidazole
Catalysis

ABSTRACT

Five new pincer type Ni(II)-Schiff base complexes of the general formula $[NiL^1(PPh_3)]$ **1**, $[NiL^2(PPh_3)]$ **2**, $[NiL^3(PPh_3)]$ **3**, $[NiL^4(PPh_3)]$ **4** and $[NiL^4(4\text{-MePy})]$ **5** [where H_2L^1 = 2-(2,3-dihydroxybenzylideneamino) phenol, H_2L^2 = N-(2,3-dihydroxybenzylidene)benzohydrazide, H_2L^3 = 2-(2,3-dihydroxybenzylidene) hydrazinecarbothioamide, H_2L^4 = 5-(diethylamino)-2-(2-hydroxybenzylideneamino)phenol, 4-MePy = 4-Methylpyridine] were synthesized by the reaction of the $Ni(OAc)_2.4H_2O$ with the corresponding Schiff base ligand in methanol as coloured crystalline solids in high yields. All the five complexes were fully characterized by FT-IR, UV–Vis, ^1H NMR, $^{13}C\{^1H\}$ NMR, $^{31}P\{^1H\}$ NMR, mass spectrometry and single crystal X-ray diffraction studies. The crystal structures of all five new complexes confirmed the tridentate nature of the pincer type Schiff base ligands (ONO and ONS) and distorted square planar geometry around the metal centre in all cases. The monodentate ligand (triphenylphosphine/4-Methylpyridine) occupied the fourth site at nickel. The catalytic potential of the complexes has been demonstrated in the synthesis of a series of 2-substituted benzimidazoles at room temperature using low catalyst loading (0.5 mol %), and without the use of any additives. All organic products were isolated in high yields (85–96%) and fully characterized by ^1H and $^{13}C\{^1H\}$ NMR studies.

1. Introduction

Nitrogen containing heterocyclic compounds are essential building blocks of numerous natural products [1], pharmaceuticals [2] and organic/polymeric materials [3]. In particular, benzimidazoles are emerged as an important class of heterocyclic system and become a significant intermediates in synthetic organic chemistry due to their miscellaneous applications [4]. Benzimidazoles are medicinally important bioactive heterocyclic scaffolds and exhibit a broad spectrum of biological and pharmacological properties including anti-bacterial [5], anti-fungal [6], anti-inflammatory [7], anti-ulcer [8], anti-cancer [9], and *anti*-HIV activities [10] (Fig. 1). The presence of imidazole ring is an integral part of several natural products such as α-amino acid histidine, proteins, histamine, purines and biotin [11]. Besides biological applications, benzimidazoles have also found applications in industry, chemical UVB filters, pigments, optical brighteners for coatings and thermostable membranes for fuel cells [12].

A Typical synthesis of benzimidazole entails the treatment of 1,2-phenylenediamine either with carboxylic acids or their derivatives under strongly acidic conditions [13] or with aldehydes under oxidative conditions using various oxidative reagents and catalysts such as $I_2/KI/K_2CO_3/H_2O$, CAN/H_2O_2, $In(OTf)_3$, $Ce(NO_3)_3.6H_2O$, $Co(OH)_2/CoO(II)$, Nano-Ni(II)/Y zeolite, Cu (II)-salen, $CuFe_2O_4$, CuO nano-particles etc. [14–34]. Although, these approaches are widely used for the synthesis of benzimidazoles, these are associated with certain drawbacks, such as formation of by-product, requirement of high reaction temperature, prolonged reaction time, expensive catalysts, toxic solvents as well as low yields of the products. In order to overcome these drawbacks, there is a need to develop a new stable, cheap catalysts capable of catalysing the synthesis of 2-substituted benzimidazoles under mild conditions.

* Corresponding author.
E-mail address: ddpathak@yahoo.com (D.D. Pathak).

https://doi.org/10.1016/j.jorganchem.2019.03.018
0022-328X/

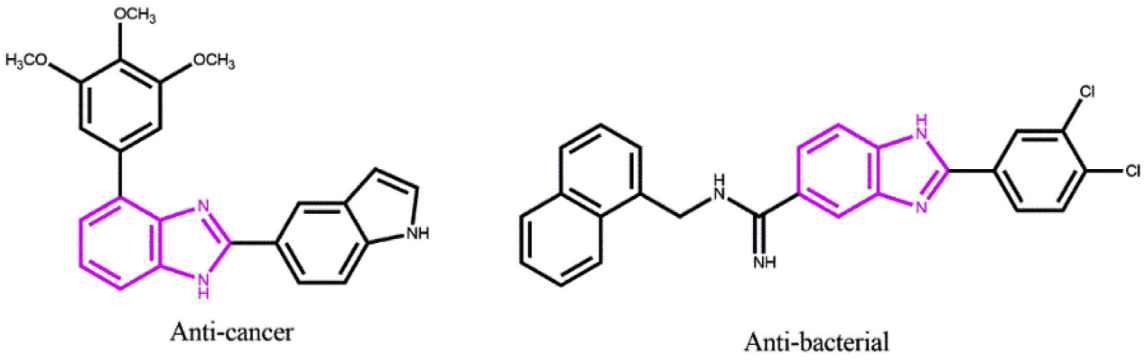

Fig. 1. Benzimidazoles moiety containing drugs.

Transition metal pincer type complexes are reported to have high stability and exhibit excellent catalytic activities in a number of homogeneous catalytic processes [35]. Tridentate pincer-type complexes have engendered a lot of interest to stabilizes a large number of metal complexes [35]. There complexes can be easily fined tuned by simple structural modifications to achieve the best catalytic activities [36]. In the area of nickel chemistry, complexes of pincer ligands have attracted considerable attention due to their low cost as compared to the precious metals, low toxicity, high reactivity and enhanced catalytic and electrochemical properties [37]. They have been successfully used as catalysts in variety of organic transformation such as C–C and C-heteroatom bond formation reactions, hydrosilylation of aldehydes and ketones, hydroamination of nitriles etc. [38]. Consequently, prompted by these results and as a continuation of our ongoing research on transition metal-catalysed organic synthesis [39], we report herein the synthesis and crystal structure of five new pincer type nickel(II)-Schiff-base complexes (**1**–**5**) having ONO and ONS donor atom and their catalytic activity in the synthesis of a series of benzimidazoles with low catalyst loading (0.5 mol %) at room temperature.

2. Results and discussion

Four Schiff base ligands H_2L^1-H_2L^4 were synthesized by the reported methods [40–43]. The ligands were obtained as red (H_2L^1), off-white (H_2L^2 and H_2L^3) and yellow (H_2L^4) solids, on refluxing ethanolic solution of corresponding aldehyde and amine for 5–8 h. The reaction of ligand H_2L^1-H_2L^4 with $Ni(OAc)_2.4H_2O$ and PPh_3/4-Methylpyridine in 1:1:1 ratio in methanol at room temperature afforded the complexes [$NiL^1(PPh_3)$] **1**, [$NiL^2(PPh_3)$] **2**, [$NiL^3(PPh_3)$] **3**, [$NiL^4(PPh_3)$] **4**, and [NiL^4(4-MePy)] **5**, respectively as a coloured crystalline solid in high yields (87–91% yields), (Scheme 1). Red block crystals suitable for X-ray crystallography were obtained by slow evaporation of the solution at room temperature in DMF. The complexes were air stable, insoluble in water and benzene, and soluble in other common organic solvents such as CH_2Cl_2, $CHCl_3$, CH_3CN, DMF and DMSO. The complexes were fully characterized by FT-IR, UV–Vis, ^1H NMR, $^{13}C\{^1H\}$ NMR, $^{31}P\{^1H\}$ NMR, mass spectrometry and their structures were determined by single crystal X-ray diffraction studies.

2.1. FT-IR spectra of ligands and complexes

The FT-IR spectral data of ligands H_2L^1-H_2L^4 and complexes **1**–**5** are given in Table 1. The FT-IR spectra of ligands H_2L^1-H_2L^4 (Fig. S1) showed band at 3369, 3480, 3532 and 3454 cm^{-1} due to presence of ν OH group and band at 1623, 1622, 1620 and 1622 cm^{-1}, were attributed to azomethine ν C=N group, respectively [44]. The FT-IR spectrum of the H_2L^2 displayed a band at 1667 cm^{-1} due to C=O group and in H_2L^3, band at 3141 cm^{-1} and 1227 cm^{-1} was due to presence of NH and C=S group, respectively. However, the FT-IR spectra of the complexes **1**–**5** showed band at 1592, 1604, 1593, 1604 and 1613 cm^{-1}, attributed to ν C=N respectively. A comparison of the spectra of ligands H_2L^1-H_2L^4 with complexes **1**–**5** indicated that in all complexes the ν C=N has been lowered by 9–31 cm^{-1}, supporting the coordination of azomethine nitrogen atom to nickel [30]. The absence of C=O stretching vibrations in complex **2** and N–H and C=S stretching vibrations in complex **3** confirms the coordination of oxygen in enol form *via* deprotonation of the –OH group and sulphur in thiol form *via* deprotonation of the –SH group to the nickel, respectively [45].

2.2. UV–vis spectra of ligands and complexes

The electronic absorption spectra of the ligands H_2L^1-H_2L^4 and complexes **1**–**5** were recorded in methanol within 200–800 nm at room temperature (Fig. S2). The electronic absorption spectra of the ligands H_2L^1-H_2L^4 showed band in the region 228–279 nm and 315–408 nm due to π-π* transitions of the aromatic rings and n-π* transitions of the azomethine group, respectively. However the electronic spectra of complexes **1**–**5** showed three absorption band in the region 307–336, 363–423, and 414–490 nm (Fig. S2). The peaks in the regions 307–336 nm were attributed to the π-π* transition. The n-π* transition corresponding to the azomethine groups observed in the range of 363–423 nm have been attributed to ligand to metal charge transfer (LMCT) transition ($^3A_{2g} \rightarrow {}^3T_{2g}$) and the shoulder at 414–490 nm to forbidden ($^3A_{2g} \rightarrow {}^3T_{1g}$) transition [46].

2.3. ^1H, $^{13}C\{^1H\}$ and $^{31}P\{^1H\}$ NMR spectra of complexes 1–5

The ^1H NMR spectra of complexes **1**–**5** were recorded in $CDCl_3$ at room temperature (Fig. S3, S7, S11, S15, S19). The ^1H NMR of ligands H_2L^1-H_2L^4 as reported [40–43] showed singlet at δ 14.19, δ 9.69 and δ 8.88 (H_2L^1), δ 11.14 and 9.20 (H_2L^2), δ 9.13 and δ 8.85 (H_2L^3), δ 14.19 and 9.58 (H_2L^4) due to presence of phenolic O*H* proton. The azomethine proton (*H*C=N-) appeared as singlet at δ 8.85, 8.58, 8.36 and 8.61 in ligands H_2L^1-H_2L^4, respectively. The phenyl proton of the free ligands were observed in the range of δ 5.91–7.93 as a complex multiplets. However, a comparision of the ^1H NMR spectra of complexes **1**–**5** with the free ligands H_2L^1-H_2L^4 exhibited upfield shift of azomethine (*H*C=N-) proton at δ 8.49, 8.36, 8.26, 8.18 and 8.49, respectively and appeared as a doublet and the phenyl protons of the ligand and PPh_3/4-Methylpyridine moieties were observed in the range of δ 7.90–5.15 as a complex multiplets [34].

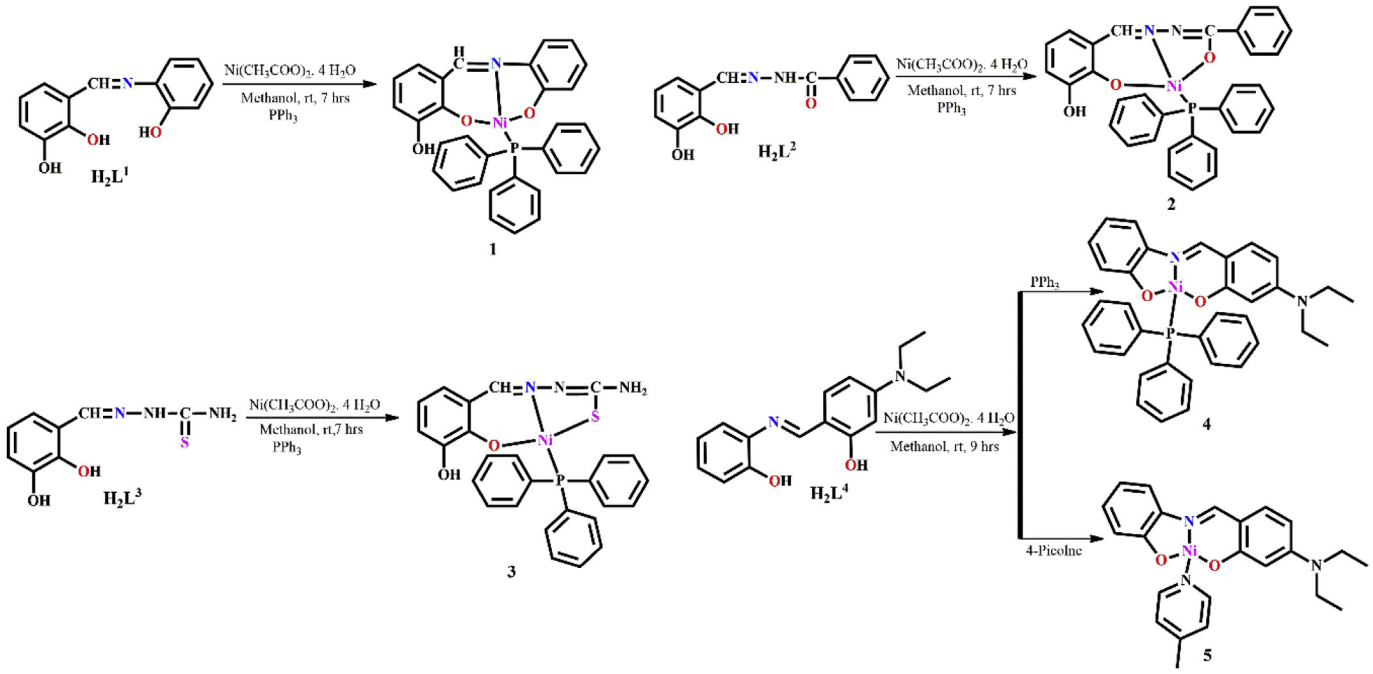

Scheme 1. Synthesis of pincer type Ni(II) complexes 1–5.

Table 1
FT-IR spectral data of ligands and nickel(II) complexes **1**–**5.**

Compound	υ OH (cm^{-1})	υ NH (cm^{-1})	υ C=O (cm^{-1})	υ C=N (cm^{-1})	υ C=S (cm^{-1})
HL^1	3369	–	–	1623	–
HL^2	3480	3291	1667	1622	–
HL^3	3532	3141	–	1620	1227
HL^4	3454	–	–	1622	–
$[NiL^1(PPh_3)]$ **1**	3443	–	–	1592	–
$[NiL^2(PPh_3)]$ **2**	3453	–	–	1604	–
$[NiL^3(PPh_3)]$ **3**	3586	–	–	1593	–
$[NiL^4(PPh_3)]$ **4**	–	–	–	1604	–
$[NiL^4$(4-MePy)] **5**	–	–	–	1613	–

Splitting of imine signal into a doublet was observed and attributed to coupling of imine proton with the phosphorus/nitrogen atom of auxiliary ligand [47]. The ^{1}H NMR spectrum of complexes **1**–**3** showed only one singlet for O*H* at *δ* 4.75, 4.93 and 4.97, respectively. The absence of other phenolic O*H* signals in complex **1**–**3** confirms the coordination of phenolic oxygen of H_2L^1-H_2L^3 to the metal ion. In complexes **4** and **5**, the CH_2 and CH_3 protons of 4-(diethylamino)-2 hydroxybenzaldehyde moiety appeared as quartet and triplet at δ 3.20 and 3.30 and δ 1.06 and 1.13, respectively [46,48].

$^{13}C\{^1H\}$ NMR spectra of the complexes **1**–**5** were recorded in $CDCl_3$ at room temperature (Fig. S4, S8, S12, S16, S20). The ^{13}C NMR spectra of complexes **1**–**5** displayed signal at 165.9, 173.3, 171.1, 164.57 and 164.723, corresponding to azomethine carbon, respectively. In complexes **2** and **3**, a signal at 173.2 and 170.9 was due to presence of N=C–O and N=C–S, carbon respectively. The signals appeared in the region of δ 113.56–150.57 (complex **1**), 149.42–113.47 (complex **2**), 152.45–113.24 (complex **3**), 151.73–93.53 (complex **4**) and 152.13–99.76 (complex **5**) were accounted to various aromatic carbons of the ligands H_2L^1-H_2L^4 as well as tripenylphosphine/4-Methylpyridine. In complexes **4**–**5**, the CH_2 and CH_3 carbon of 4-(diethylamino)-2-hydroxybenzaldehyde appeared at 44.82, 44.3 and 13.27, 12.8 respectively and the signal at 21.02 in complex **5** was attributed to methyl carbon of 4-Methylpyridine [49].

The $^{31}P\{^1H\}$ NMR spectra of complexes **1**–**4** were recorded in $CDCl_3$ at room temperature (Fig. S5, S9, S13, S17). The $^{31}P\{^1H\}$NMR spectra of complexes **1**–**4** showed a singlet at δ 16.29, δ 19.17, δ 23.93 and δ 26.87, respectively. The free PPh_3 ligand exhibit a resonance at δ −6.4. The downfield shifting of the resonance clearly indicates the coordination of the PPh_3 ligand [50].

2.4. Single crystal X-ray studies

Diffraction quality crystals of the complexes (**1**–**5**) were grown over a period of two weeks by standing a concentrated solution of the complex in DMF at room temperature. A summary of the crystallographic and refinement data of complexes **1**–**5** are given in Table 2. The structures of the complexes, **1**–**5** have been elucidated by single-crystal X-ray diffraction studies and the ORTEP diagram of the complexes are shown in Fig. 2. ORTEP structure and crystallographic and refinement data reveals that complexes crystallizes in triclinic (**1** and **4**) and monoclinic (**2**, **3** and **5**) system, and consist of tridentate ligand and PPh_3/4-Methylpyridine. The ligand is coordinated through the ONO/ONS donor atom and fourth coordination site was occupied by phosphorous/nitrogen atom forming four-coordinated species with distorted square planar geometry. Distortion is mainly caused by the presence of the doubly deprotonated tridentate Schiff base ligand, which forms one five-

Table 2
Crystal data and refinement parameters of complexes **1**–**5.**

CCDC	1473738	1526857	1585092	1536826	1537251
Chemical formula	$C_{31}H_{24}NNiO_3P$	$C_{32}H_{25}N_2NiO_3P$	$C_{29}H_{28}N_4NiO_3PS$	$C_{35}H_{33}N_2NiO_2P$	$C_{23}H_{25}N_3NiO_2$
Formula weight	548.19 g/mol	575.22 g/mol	602.29 g/mol	603.31 g/mol	434.17 g/mol
Temperature	103(2) K	103(2) K	203(2) K	296 K	296 K
Wavelength	1.54178 Å	1.54178 Å	0.71073 Å	0.71073 Å	0.71073 Å
Crystal size	0.100 × 0.140 × 0.220 mm	0.160 × 0.060 × 0.040 mm	0.140 × 0.220 × 0.280 mm	0.37 × 0.31 × 0.23 mm	0.62 × 0.45 × 0.32 mm
Crystal habit	red block	red block	red block	red block	red block
Crystal system	triclinic	monoclinic	monoclinic	triclinic	monoclinic
Space group	*P -1*	*P 1 21/n 1*	*P 1 21/n 1*	*P1*	*P21/n*
Unit cell dimensions					
a (Å)	76.3139(5)°	90°	90°	82.472 (4)°	90°
β (Å)	88.3431(5)°	101.4877(12)°	102.702(16)°	75.563 (4)°	101.269°
γ (Å)	76.5697(5)°	90°	90°	74.087 (4)°	90°
a	8.98080(10) Å	15.7729(3) Å	9.960(3) Å	10.1793 (6) Å	10.5869 Å
b	10.01310(10) Å	15.3705(2) Å	15.038(4) Å	15.6331 (8) Å	7.6769 Å
c	14.4375(2) Å	22.1748(3) Å	19.637(6) Å	20.4722 (10) Å	26.0646 Å
Volume	1226.48(3) $Å^3$	5268.31(14) $Å^3$	2869.2(15) $Å^3$	3027.2 (3) $Å^3$	2077.5 (3) $Å^3$
Z	2	8	4	4	4
Density (calculated)	1.484 g/cm^3	1.450 g/cm^3	1.394 g/cm^3	1.324 Mg m^{-3}	1.388 Mg m^{-3}
Absorption coefficient	2.043 mm^{-1}	1.942 mm^{-1}	0.842 mm^{-1}	0.73 mm^{-1}	0.96 mm^{-1}
F(000)	568	2384	1252	1264	912
Goodness-of-fit on F^2	1.064	1.001	1.026	0.938	1.053
Δ/σ_{max}	0.001	0.001	0.001	0.001	0.001
Final R indices $I > 2\sigma(I)$	$R_1 = 0.0349$, $wR_2 = 0.0899$	$R_1 = 0.0609$, $wR_2 = 0.1402$,	$R_1 = 0.0541$, $wR_2 = 0.1140$,	$R_1 = 0.0392$, $wR_2 = 0.0951$	$R_1 = 0.0440$, $wR_2 = 0.1268$
R indices (all data)	$R_1 = 0.0366$, $wR_2 = 0.0932$	$R_1 = 0.1040$, $wR_2 = 0.1638$	$R_1 = 0.0978$, $wR_2 = 0.1324$	$R_1 = 0.0640$, $wR_2 = 0.1018$	$R_1 = 0.0512$, $wR_2 = 0.1314$

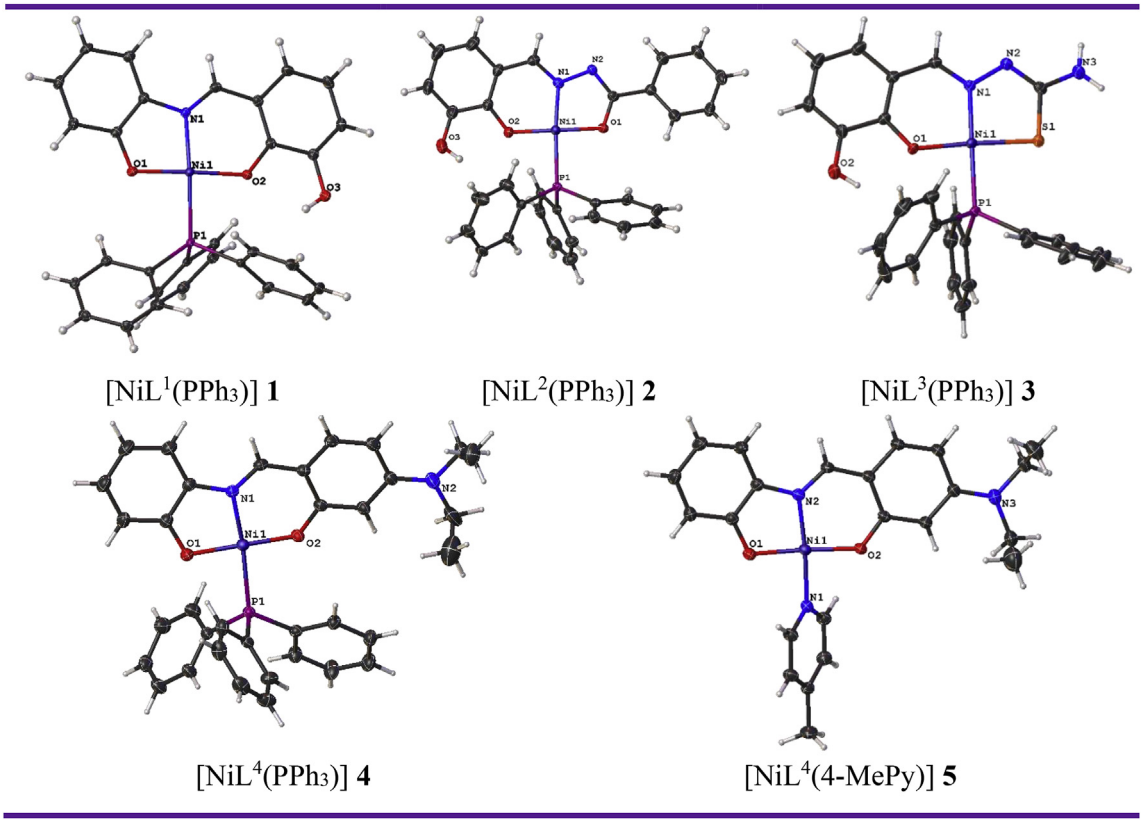

Fig. 2. ORTEP diagram of [$NiL^1(PPh_3)$] **1,** [$NiL^2(PPh_3)$] **2,** [$NiL^3(PPh_3)$] **3** (DMF molecule omitted, [$NiL^3(PPh_3)$] **4** and [NiL^4(4-MePy)] **5** complexes.

membered and one six-membered ring with nickel atom. Selected bond distances and bond angle are given in Table S1. In complexes **1**–**5,** bond angles O1–Ni–N1 are 86.84(6), 83.70(12), 95.08(11), 86.63(9) and 175.86(3), O1–Ni–P1 and N1–Ni–P1 in complexes **1**–**4** are 91.31(4), 91.39(9), 86.09(8), 86.72(6) and 173.81(5), 174.76(10), 176.13(8), 169.45(6) respectively. In complexes **3** and **5**, the bond angles O1–Ni1–S1, N1–Ni1–S1 and N2–Ni–N1 are 176.89(8), 87.65(8) and 174.57(10), respectively. The Ni(1)–O(1) and Ni(1)–N(1) bond lengths in complexes **1**–**5** are 1.836(13), 1.842(2), 1.856(2), 1.838(18), 1.839(2) and 1.888(15), 1.848(3),

1.894(3), 1.874(2), 1.914(2), respectively which are in close agreement with the previously reported Ni(II) complexes [45]. In complex **5**, Ni(1)–S(1) bond length is 2.124(11) is nearly similar to previously reported Ni(II) complex published by K. Natarajan et al. having Ni–S bond length 2.127 [46].

2.5. Catalytic studies

All the complexes were screened for their catalytic activity in the synthesis of 2-substituted benzimidazoles (Scheme 2). Initially benzaldehyde and *o*-phenylenediamine were chosen as model substrates. Various parameters such as catalyst loading, solvent and time were studied and optimized. The results are summarised in Table 3. When the reaction was carried out in absence of catalyst in ethanol at room temperature, 10% yield of the product was observed after 12 h (Table 3, entry 1). However, in presence of 0.2 mol % of catalyst **1**, 75% yield of the desired product was obtained in 5 h (Table 3, entry 2). Further, increasing the catalyst loading from 0.2 mol % to 0.5 mol % and 0.8 mol % resulted in 94% yield of the desired product in 2h (Table 3, entries 3–4). Thus 0.5 mol % of catalyst loading was found to be optimum. The reaction was also performed using complexes **2**–**5** as catalyst, (Table 3, entries 3–8). Complex **1** and complex **2** showed superior catalytic activity towards benzimidazoles synthesis. The lower catalytic activity of complexes **3** (ONS) may be due to larger atomic (or Van der Waals) radius of sulphur atom which may lower the activity of the catalyst due to steric effect [51]. Presence of electron donating group at para position of aldehyde in complex **4** and weaker σ-donor properties of 4-methylpyridine in complex **5** may be the reason for the lower catalytic activity [52]. In order to found the best solvent, the reaction was carried out in different solvents such as EtOH, MeOH, $CHCl_3$, CH_3CN and DMF (Table 3). Among all solvents, EtOH gave the best yield of product and was found to be the best solvent (Table 3, entry 3). Thus, the optimal reaction conditions and best yield (94%) was achieved in the presence of 0.5 mol% of complex **1** in ethanol solvent at room temperature within 2 h (Table 3, entry 3).

Subsequently, all reactions were carried out under optimized conditions with a structurally diverse range of aldehydes to give corresponding benzimidazoles (Table 4). It can be concluded that the nature of substituent such as electron donating and electron withdrawing group on aldehyde resulted in good yield. However aldehydes containing electron-withdrawing groups (Br, Cl, F, NO_2) gave products in higher yields than those containing electron-donating groups (CH_3, OCH_3, OH) (Table 4, entries 4b-4j). This may be due to increase in the electrophilicity of the carbonyl carbon of aldehydes by the electron withdrawing group [53]. The *para*- and *meta*-substituted aldehydes resulted in good yield as compared to substituent at ortho position (Table 4). This may be due to steric effect. The reaction with heteroaromatic aldehydes i.e. quinoline-2-carbaxaldehyde and thiophene-2-carbaxaldehyde resulted in good yield of the desired product (Table 4, entry 4k-l). The isolated products were fully characterized by ^1H and ^{13}C NMR as given in ESI (Fig. S22-S33). In order to establish the efficacy of the new catalysts, a comparison was made with some previously reported catalysts for 2-substituted benzimidazole synthesis in terms of catalyst loading, temperature, time [16–18,20,32,34] etc. (Table 5). The results indicate that our catalytic system exhibits better catalytic activity as compared to other reported catalyst.

Table 3
Optimization of reaction conditions for synthesis of benzimidazoles[a].

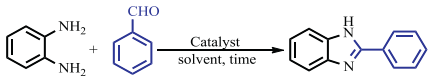

Entry	Catalyst	Catalyst loading (mol %)	Solvent	Time	Yield[b] (%)
1	–	–	EtOH	12	10
2	Complex 1	0.2	EtOH	5	75
3	Complex 1	0.5	EtOH	2	94
4	Complex 1	0.8	EtOH	2	94
5	Complex 2	0.5	EtOH	2	93
6	Complex 3	0.5	EtOH	2	82
7	Complex 4	0.5	EtOH	2	89
8	Complex 5	0.5	EtOH	2	85
9	Complex 1	0.5	MeOH	3	75
10	Complex 1	0.5	$CHCl_3$	4	45
11	Complex 1	0.5	CH_3CN	4	58
12	Complex 1	0.5	DMF	4	84

[a] Reaction conditions: Aldehyde (1 mmol), *o*-phenylenediamines (1 mmol), RT.
[b] Yield after column chromatography.

A plausible mechanism for benzimidazoles synthesis, based on previous reports [19,54,55] is suggested in Scheme 3. Initially triphenylphosphine ligand dissociate from the complex to provide a coordination centre [50,56]. Further, the reaction presumably proceeds *via* activation of aldehyde by Ni(II) followed by imine formation and the resulting imine further reacts with another $-NH_2$ group of 1,2-phenylenediamine resulting in the formation of dihydroimidazole. Subsequently dihydroimidazole undergoes aromatization under aerial oxidation to give benzimidazole.

3. Conclusion

In conclusion, five new pincer type Ni(II)-Schiff-base complexes **1**–**5**, have been synthesized and characterized by various spectroscopic techniques and structure of the complexes was confirmed by single crystal X-ray structure determination. The catalytic application of Ni(II) complexes has been demonstrated in the synthesis of a series of 2-substituted benzimidazoles from various aldehydes and *o*-phenylenediamine. Complex **1** and complex **2** showed superior catalytic activity than complexes **3**–**5** towards benzimidazoles synthesis as high yields of product were obtained with these complexes. The reactions proceeded smoothly at a low catalyst loading at room temperature without use of additives and base.

4. Experiment

4.1. Materials and instrumentations

All reagents and solvents for the synthesis and analysis were purchased from Merck and Sigma Aldrich and used as received without further purifications.

FT-IR spectra were recorded on a Perkin Elmer Spectrometer in the range of 400–4000 cm^{-1} using KBr pellets. Electronic

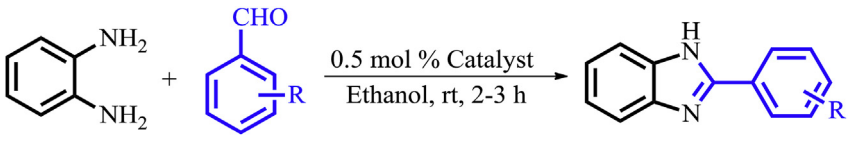

Scheme 2. The catalytic activity of Ni(II) complexes in benzimidazoles synthesis.

Table 4
The reaction of various aldehydes with *o*-phenylenediamines under optimized reaction conditions[a,b].

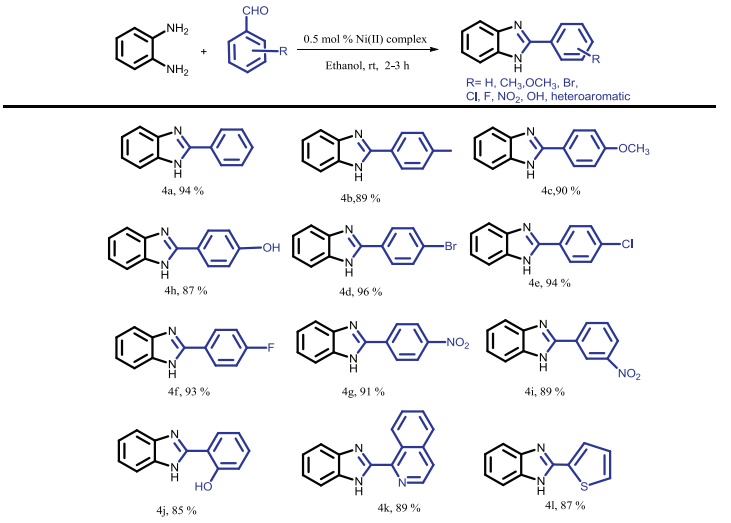

[a]Reaction conditions: Aldehyde (1 mmol) and *o*-phenylenediamines (1 mmol).
[b]Yield after column chromatography.

Table 5
A comparison study of synthesized Ni(II) complex with the previous reported catalysts for benzimidazole synthesis.

Entry	Catalyst	Catalyst loading (mol %)	Temperature (°C)	Time (h)	Yields (%)	Reference
1	Cu(II)-salen	5	50	3	90	[34a]
2	$CuFe_2O_4$ nanoparticle	50	110	24	89	[34b]
3	$Zn(OTf)_2$	10	80	8	95	[32]
4	MoO_3	2	50	0.5	93	[34c]
5	$Co(OH)_2$/CoO(II)	10	rt	4–9	98	[18]
6	$Ce(NO_3)_3 \cdot 6H_2O$	30	80	1.5–6	94	[17]
7	$In(OTf)_3$	5	rt	0.5	95	[16]
8	$Ni(NO_3)_2.6H_2O$	50	80	0.5	89	[20]
9	Pincer Ni(II) Complexes	0.5	rt	2–3	96	This work

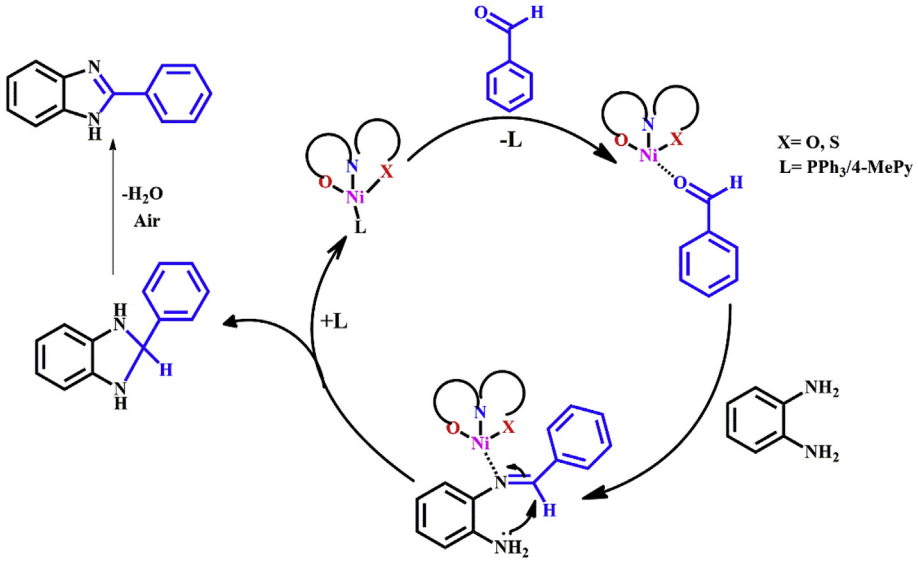

Scheme 3. Plausible mechanism for benzimidazole synthesis.

absorption spectral analysis was recorded on a Shimadzu UV-1800 Spectrophotometer in the wavelength range of 200–800 nm. The ^1H and ^{13}C NMR spectra of the isolated products were recorded on a Bruker AvIII HD-400 MHz spectrometer in DMSO-d_6 using TMS as the internal Standard. Melting points were recorded on a Yazawa micro melting point apparatus.

4.2. General synthesis of Ni(II) complexes 1-5

The H_2L^1-H_2L^4 was synthesized by the reported method [40–43]. A solution of the corresponding ligand H_2L^1-H_2L^4 (0.50 mmol) in 2 mL methanol was added drop-wise to the methanolic solution of $Ni(OAc)_2.4H_2O$ (0.50 mmol, 4 mL) with constant stirring at room temperature. After stirring the solution for 10 min, PPh_3/4-Methylpyridine (0.50 mmol) dissolved in 2 mL methanol was added *via* a syringe to the reaction. After 6–9 h of stirring at room temperature, the resultant precipitate was filtered, washed with cold ethanol and dried in vacuum over anhydrous $CaCl_2$. The precipitate was re-crystallized from DMF. Suitable single crystals for X-ray crystallography were grown over a period of two weeks from a concentrated solution of the complex in DMF.

[$NiL^1(PPh_3)$] **1**: Yield: 0.495 g, 91%,. FT-IR (KBr), cm^{-1}: 3443 ν (OH), 1592 ν (C═N), 3056 ν (CH_{ar}), 1474 ν (C=C_{ring}), 517 ν (Ni–O), 443 ν (Ni–N). ^{1}H NMR ($CDCl_3$, 25 °C, 400 MHz): δ 8.49 (d, 1H, *H*–CN), δ 7.90–7.86 (m, 6H, Ar *H*), 7.72–7.70 (m, 1H, Ar *H*), 7.55–7.46 (m, 9H, Ar *H*), 7.00–6.94 (m, 2H, Ar *H*), 6.65–6.64 (m, 2H, Ar *H*), 6.59–6.53 (m, 2H, Ar *H*), δ 4.74 (s,1H,O*H*).^{13}C{^{1}H} NMR($CDCl_3$,25 °C,100 MHz):δ 165.99, 150.57, 148.58, 134.47, 132.15, 130.99, 128.81, 122.90, 119.39, 118.06, 116.02, 114.83, 114.20,113.56, ^{31}P{^{1}H}NMR ($CDCl_3$, 25 °C, 160 MHz): δ 16.29. ESI-MS (ES^+; *m*/*z*): Calculated for $C_{31}H_{24}NNiO_3P$ 548.19, Found 548.11.

[$NiL^2(PPh_3)$] **2**: Yield: 0.500 g, 87%,. FT-IR (KBr), cm^{-1}: 3455 ν (OH), 1524 ν (C═N), 3052 ν (CH_{ar}), 1213 ν (C–O), 1433 ν (C=C_{ring}), 508 ν (Ni–O), 426 ν (Ni–N). ^{1}H NMR ($CDCl_3$, 25 °C, 400 MHz): δ 8.35 (d, 1H, *H*–CN), δ 7.86–7.81 (m, 6H, Ar *H*), 7.73–7.72 (m, 2H, Ar *H*), 7.55–7.54 (m, 9H, Ar *H*), 7.49–7.47 (m, 3H, Ar *H*) 7.25–7.23 (m, 1H, Ar *H*), 6.91–6.53 (m, 2H, Ar *H*), δ 4.92 (s,1H, O*H*). ^{13}C{^{1}H} NMR ($CDCl_3$, 25 °C, 100 MHz):δ 173.30, 173.20, 149.43, 148.96, 147.84,134.57, 134.37, 134.26,131.15,139.6,130.25, 128.96, 128.87, 128.15,128.00, 122.15, 118.24,116.09, 113.07, ^{31}P{^{1}H}NMR ($CDCl_3$, 25 °C, 160 MHz): δ 19.17. ESI-MS (ES^+; *m*/*z*): Calculated for $C_{32}H_{25}N_2NiO_3P$ 575.22, found 575.12

[$NiL^3(PPh_3)$] **3**: Yield: 0.536 g, 89%. FT-IR (KBr), cm^{-1}: 3432–3350 ν (NH_2), 3577 ν (OH), 1593 ν (C═N). ^{1}H NMR ($CDCl_3$, 25 °C, 400 MHz): δ 8.26 (d, 1H, *H*–CN), δ 8.24 (s, 1H, Ar *H*), δ 7.83–7.78 (m, 6H, Ar *H*), 7.55–7.52 (m, 3H, Ar *H*), 7.48–7.44 (m, 5H, Ar *H*), 6.84–6.81 (m, 1H, Ar *H*), 6.69–6.67 (m, 1H, Ar *H*), 6.55–6.49 (m, 1H, Ar *H*), δ 4.97 (s,1H, O*H*), δ 4.59 (s,1H,N*H*$_2$).^{13}C{^{1}H} NMR($CDCl_3$,25 °C,100 MHz):δ 171.10, 170.99, 152.45, 149.00, 147.16, 134.37, 134.26, 131.23,128.91, 128.77,128.67, 128.44,122.33, 116.46, 115.62, 113.00, ^{31}P{^{1}H} NMR ($CDCl_3$, 25 °C, 160 MHz): δ 23.93. ESI-MS (ES^+; *m*/*z*): Calculated for $C_{26}H_{22}N_3NiO_2PS$ 529.19, found 530.08

[$NiL^4(PPh_3)$] **4**: Yield: 0.536 g, 88%. FT-IR (KBr), cm^{-1}: 1604 ν (C═N), 2975 ν (CH_{ar}), 1468 ν (C=C_{ring}). ^{1}H NMR ($CDCl_3$, 25 °C, 400 MHz): δ 8.18 (d, 1H, *H*–CN), δ 7.88 (m, 10H, Ar *H*), 7.58–7.57 (m, 2H, Ar *H*), 7.03 (m, 3H, Ar *H*), 6.85–6.84 (m, 1H, Ar *H*), 6.56–6.50 (m, 3H, Ar *H*), 6.12–6.10 (m, 1H, Ar *H*), 5.32–5.28 (m, 2H, Ar *H*), 5.15 (m, 1H, Ar *H*), 3.24–3.15 (q, 4H, $-CH_2$)), δ 1.06–1.04 (t, 6H, $-CH_3$). ^{13}C {^{1}H}NMR($CDCl_3$,25 °C,100 MHz):δ 164.57, 151.73, 149.88, 147.13, 135.13, 134.43, 130.70, 128.61, 126.92, 117.85, 114.25, 113.38,104.04, 100.90, 93.53, 44.82, 13.27.^{31}P{^{1}H} NMR ($CDCl_3$, 25 °C, 160 MHz): δ 26.87. ESI-MS (ES^+; *m*/*z*): Calculated for $C_{35}H_{33}N_2NiO_2P$ 603.31, Found 604.17.

[NiL^4(4-MePy)] **5**: Yield: 0.376 g, 87%. FT-IR (KBr), cm^{-1}: 1613 ν (C═N), 2975 ν (CH_{ar}), 1486 ν (C=C_{ring}). ^{1}H NMR ($CDCl_3$, 25 °C, 400 MHz): δ 8.49 (d, 1H, *H*–CN), δ 7.77 (d, 1H, Ar *H*), δ 7.42–7.39 (m, 1H, Ar *H*), 7.15–7.13 (m, 3H, Ar *H*), 6.86–6.83 (m, 1H, Ar *H*), 6.65–6.63 (m, 1H, Ar *H*), 6.47–6.43 (m, 1H, Ar *H*), 6.17–6.14 (m, 1H, Ar *H*), 6.03 (m, 1H, Ar *H*), 3.34–3.29 (q, 4H, $-CH_2$), 1.15–1.12 (t, 6H, $-CH_3$). ^{13}C{^{1}H} NMR(CDCl3, 25^{O}C, 100 MHz): 164.72, 163.66, 152.13, 149.95, 133.91, 126.82, 125.10,116.70, 114.33, 133.13, 112.19, 112.9, 103.89, 99.76, 44,37, 21.02, 12.86. ESI-MS (ES^+; *m*/*z*): Calculated for $C_{23}H_{25}N_3NiO_2$ 434.17, Found 434.15.

4.3. General procedure for the synthesis of 2-substituted benzimidazoles

A mixture of aldehyde (1.0 mmol) and *o*-phenylenediamine (1.0 mmol) and complex **1** (0.5 mol %) was stirred at room temperature in ethanol (5 mL) for 2–3 h. The progress of the reaction was monitored by TLC. After completion of the reaction, the solvent was removed and the product washed with water and extracted with ethyl acetate (3 × 10 mL). The combined organic layers were dried over Na_2SO_4 and the solvent removed under reduced pressure to give crude product which was purified by column chromatography by using petroleum ether/ethyl acetate as an eluent. The products were confirmed by ^{1}H and ^{13}C NMR.

4.4. Crystallographic studies

The X-ray diffraction data were collected on a Bruker Kappa diffractometer at 103(2) K (complexes **1**–**2**), 203(2) K (complex **3**) and 296 K (complexes **4**–**5**) equipped with a CCD detector, employing Cu radiation (complex 1–2) and Mo K α radiation (complex 3–5) (λ = 1.54178 Å (complex 1–2) and 0.71073 Å (complexes 3–5), with the SMART suite of programs [57]. All data were processed and corrected for Lorentz and polarization effects with SAINT and for absorption effects with SADABS [58]. Structural solution and refinement were carried out with the SHELXTL suite of programs [59]. The structures were refined (weighted least squares refinement on F^2) to convergence. All the non-hydrogen atoms in all the compounds were refined anisotropically by full-matrix least-squares refinement. A summary of the crystallographic and refinement data of complexes **1**–**5** are given in Table 2.

Acknowledgments

We are thankful to the CRF IIT (ISM), SAIF Panjab University, Chandigarh and IISER Bhopal for providing help in the analysis of the samples. Bhumika Agrahari and Samaresh Layek acknowledges the receipt of IIT (ISM) fellowship.

Appendix A. Supplementary data

Supplementary data related to this article can be found at https://doi.org/10.1016/j.jorganchem.2019.03.018.

References

[1] E. Vitaku, D.T. Smith, J.T. Njardarson, J. Med. Chem. 57 (2014) 10257–10274.
[2] (a) A.P. Taylor, R.P. Robinson, Y.M. Fobian, D.C. Blakemore, L.H. Jones, O. Fadey, Org. Biomol. Chem. 14 (2016) 6611–6637;
(b) C.D. Hadole, J.D. Rajput, R.S. Bendre, Org. Chem. Curr. Res. 7 (2018) 3.
[3] J.A. Asensio, E.M. Sanchez, P. Gomez-Romero, Chem. Soc. Rev. 39 (2010) 3210–3239.
[4] (a) Y. Bansal, O. Silakari, Bioorg. Med. Chem. 20 (2012) 6208–6236;
(b) L.Y. Zhang, S.Y. Yin, M. Pan, W.M. Liao, J.H. Zhang, H.P. Wang, C.Y. Su, J. Mater. Chem. 5 (2017) 9807–9814;
(c) C. Yan, Y.Z. Fan, L. Chen, M. Pan, L.Y. Zhang, J.J. Jiang, C.Y. Su, CrystEngComm 17 (2015) 546–552;
(d) S.R. Zheng, M. Pan, K. Wu, L. Chen, J.J. Jiang, D.W. Wang, J.Y. Shi, C.Y. Su, Cryst. Growth Des. 15 (2015) 625–634.
[5] P.S. Hameed, A. Raichurkar, P. Madhavapeddi, S. Menasinakai, S. Sharma, P. Kaur, R. Nandishaiah, V. Panduga, J. Reddy, V.K. Sambandamurthy, D. Sriram, ACS Med. Chem. Lett. 5 (2014) 820–825.
[6] B. Fang, C.H. Zhou, X.C. Rao, Eur. J. Med. Chem. 45 (2010) 4388–4398.
[7] (a) S.N.A. Bukhari, G. Lauro, I. Jantan, C.F. Chee, M.W. Amjad, G. Bifulco, H. Sher, I. Abdullah, N.A. Rahman, Future Med. Chem. 8 (2016) 1953–1967;
(b) G. Kaur, M. Kaur, O. Silakari, Mini Rev. Med. Chem. 14 (2014) 747–767.
[8] G. Yadav, S. Ganguly, Eur. J. Med. Chem. 97 (2015) 419–443.
[9] (a) J.S. Kim, B. Gatto, C. Yu, A. Liu, L.F. Liu, E.J. LaVoie, J. Med. Chem. 39 (1996) 992–998;

(b) A. Husain, M. Rashid, R. Mishra, S. Parveen, D.S. Shin, D. Kumar, Bioorg. Med. Chem. Lett 22 (2012) 5438–5444;
(c) A. Husain, M. Rashid, M. Shaharyar, A.A. Siddiqui, R. Mishra, Eur. J. Med. Chem. 62 (2013) 785–798.
[10] (a) T. Roth, M.L. Morningstar, P.L. Boyer, S.H. Hughes, R.W. Buckheit Jr., C.J. Michejda, J. Med. Chem. 40 (1997) 4199–4207;
(b) M.L. Morningstar, T. Roth, D.W. Farnsworth, M.K. Smith, K. Watson, R.W. Buckheit, J.K. Das, W. Zhang, E. Arnold, J.G. Julias, S.H. Hughes, C.J. Michejda, J. Med. Chem. 50 (2007) 4003–4015.
[11] R.S. Keri, A. Hiremathad, S. Budagumpi, B.M. Nagaraja, Chem. Biol. Drug Des. 86 (2015) 19–65.
[12] (a) P. Fritsch, Dermatologie und Venerologie, vol 2, Springer-Verlag, Berlin, 2004, p. 171;
(b) H.M. Smith, High Performance Pigments, Wiley-VCH Verlag GmbH & Co. KGaA, Weinheim, Germany, 2002, pp. 135–158;
(c) B. Meuthen, A.S. Jandel, Coil Coating, 2. Auflage, Friedr, Vieweg & Sohn Verlag, Wiesbaden, Germany, 2008, p. 65;
(d) G.G. Scherer, Fuel Cells II, Springer-Verlag, Berlin, 2008, pp. 65–120.
[13] (a) E.C. Wagner, W.H. Millett, Org. Synth. 19 (1939), 12-12;
(b) L.C.R. Carvalho, E. Fernandes, M.M.B. Marques, Chem. Eur J. 17 (2011) 12544–12555;
(c) J.B. Wright, Chem. Rev. 48 (1951), 397-541;
(d) P.N. Preston, Chem. Rev. 74 (1974) 279–314;
(e) K.J. Lee, K.D. Janda, Can. J. Chem. 79 (2001) 1556–1561;
(f) M. Curini, F. Epifano, F. Montanari, O. Rosati, S. Taccone, Synlett (2004) 1832–1834;
(g) P.L. Beaulieu, B. Haché, E. Von Moos, Synthesis 11 (2003) 1683–1692;
(h) Y.X. Chen, L.F. Qian, W. Zhang, B. Han, Angew. Chem. Int. Ed. 47 (2008) 9330–9333.
[14] P. Gogoi, D. Konwar, Tetrahedron Lett. 47 (2006) 79–82.
[15] K. Bahrami, M.M. Khodaei, F. Naali, J. Org. Chem. 73 (2008) 6835–6837.
[16] R. Trivedi, S.,K. De, R.A. Gibbs, J. Mol. Catal. A Chem. 245 (2006) 8–11.
[17] G.M. Martins, T. Puccinelli, R.A. Gariani, F.R. Xavier, C.C. Silveira, S.R. Mendes, Tetrahedron Lett. 58 (2017) 1969–1972.
[18] A.C. Murugulla, S. Donthabhakthuni, T. Sasaki, Tetrahedron Lett. 52 (2011) 5575–5580.
[19] (a) A. Mobinikhaledi, M. Zendehdel, F. Goudarzi, G.R. Bardajee, Syn. React. Inorg. M. 46 (2016) 1526–1531;
(b) L.H. Du, Y.G. Wang, 2007, Synthesis (2007) 675–678.
[20] C.D. Shendkar, P.S. Chandrachood, T.V. Gadakari, R.C. Torane, N.R. Deshpande, J. Pharm. Res. 4 (2011) 4780–4782.
[21] K. Bahrami, M.M. Khodaei, I. Kavianinia, 2007, Synthesis (2007) 547–550.
[22] S. Lin, S.L. Yang, Tetrahedron Lett. 46 (2005) 4315–4319.
[23] R. Nagawade, D.B. Shinde, Chin. Chem. Lett. 17 (2006) 453–456.
[24] H. Hashem, H.S. Mona, M. Fatemeh, Can. J. Chem. 86 (2008) 1044–1051.
[25] A. Chari, P. Sadanandam, D. Shobha, K. Mukkanti, J. Heterocycl. Chem. 47 (2010) 153–155.
[26] A.T. Khan, T. Parvin, L.H. Choudhury, Synth. Commun. 39 (2009) 2339–2346.
[27] U. Srinivas, C. Srinivas, P. Narender, V.J. Rao, S. Palaniappan, Catal. Commun. 8 (2007) 107–110.
[28] S.M. Inamdar, V.K. More, S.K. Mandal, Tetrahedron Lett. 54 (2013) 579–583.
[29] M. Curini, F. Epifano, F. Montanari, F.O. Rosati, S. Taccone, 2004, Synlett (2004) 1832–1834.
[30] H. Sharghi, O. Asemani, S.M.H. Tabaei, J. Heterocycl. Chem. 49 (2009) 1293.
[31] A. Mobinikhaledi, N. Forughifar, M. Zendehdel, M. Jabbarpour, Synth. React. Inorg. Metal-Org. Nano-Metal Chem. 38 (2008) 390–393.
[32] R. Srinivasulu, K.R. Kumar, P.V.V. Satyanarayana, Green Sustain. Chem. 4 (2014) 33–37.
[33] (a) D.S. Chandrakant, S.C. Pranav, V.G. Tushar, C.T. Rasika, R.D. Nirmala, J. Pharm. Res 12 (2011) 4780–4782;
(b) M. Karthik, P. Suresh, New J. Chem. 42 (2018) 17931–17938;
(c) A. Chakraborty, S. Bhattacharyya, A. Hazra, A.C. Ghosh, T.K. Maji, Chem. Commun. 52 (2016) 2831–2834;
(d) Q. Luo, Z. Dai, H. Cong, R. Li, T. Peng, J. Zhang, Dalton Trans. 46 (2017) 15012–15022.
[34] (a) H. Sharghi, M. Aberi, P. Shiri, Appl. Organomet. Chem. 31 (2017), 3761-3674;
(b) D. Yang, X. Zhu, W. Wei, N. Sun, L. Yuan, M. Jiang, J. You, H. Wang, RSC Adv. 4 (2014) 17832–17839;
(c) M. Jafarpour, A. Rezaeifard, M. Ghahramaninezhad, T. Tabibi, New J. Chem. 37 (2013) 2087–2095.
[35] N. Selander, K.J. Szabo, Chem. Rev. 111 (2011) 2048–2076.
[36] D. Morales-Morales, in: C.M. Jensen (Ed.), Elsevier, Amsterdam, 2007.
[37] Z.X. Wang, N. Liu, 2012, Eur. J. Inorg. Chem. (2012) 901–911.
[38] (a) K. Inamoto, J. Kuroda, K. Hiroya, Y. Noda, M. Watanabe, T. Sakamoto, Organometallics 25 (2006) 3095–3098;
(b) P. Hasche, M. Joksch, G. Vlachopoulou, H. Agarwala, A. Spannenberg, T. Beweries, 2018, Eur. J. Inorg. Chem. (2018) 676–680;
(c) G.T. Venkanna, S. Tammineni, H.D. Arman, Z.J. Tonzetich, Organometallics 32 (2013) 4656–4663;
(d) S. Chakraborty, J.A. Krause, H. Guan, Organometallics 28 (2009) 582–586;
(e) Z. Yang, D. Liu, Y. Liu, M. Sugiya, T. Imamoto, W. Zhang, Organometallics 34 (2015) 1228–1237.
[39] (a) B. Agrahari, S. Layek, S. Kumari, Anuradha, R. Ganguly, D.D. Pathak, J. Mol. Struct. 1134 (2017) 85–90;
(b) S. Layek, S. Kumari, Anuradha, B. Agrahari, R. Ganguly, D.D. Pathak, Inorg. Chim. Acta 453 (2016) 735–741;
(c) S. Layek, Anuradha, B. Agrahari, D.D. Pathak, J. Organomet. Chem. 846 (2017) 105–112;
(d) S. Layek, B. Agrahari, S. Kumari, Anuradha, D.D. Pathak, Catal. Lett. 148 (2018) 2675–2682;
(e) B. Agrahari, S. Layek, S. Kumari, Anuradha, R. Ganguly, D.D. Pathak, Inorg. Chim. Acta 471 (2018) 345–354;
(f) B. Agrahari, S. Layek, R. Ganguly, D.D. Pathak, New J. Chem. 42 (2018) 13754–13762;
(g) A. Kumar, S. Layek, B. Agrahari, S. Kujur, D.D. Pathak, Chem. Select 4 (2019) 1337–1345.
[40] T.F.F. Magalhaes, C.M. da Silva, A. de Fatima, D.L. da Silva, L.V. Modolo, C.V.B. Martins, R.B. Alves, A.L.T.G. Ruiz, G.B. Longato, J.E. de Carvalho, M.A.D.R. Stoianoff, Lett. Appl. Microbiol. 57 (2013) 137–143.
[41] (a) H.M. Ali, S. Puvaneswary, W.J. Basirun, S.W. Ng, Acta Crystallogr. 61 (2005) 1013–1014;
(b) M. Nandy, S. Shit, C. Rizzoli, G. Pilet, S. Mitra, Polyhedron 88 (2015) 63–72.
[42] A.T. Swesi, Y. Farina, I. Baba, Sains Malays. 36 (2007) 21–26.
[43] A. Neeraj, V. Kumar, R. Kumar, S. Prajapati, Asthana Kumar, K.K. Upadhyay, J. Zhao, Dalton Trans. 43 (2014) 5831–5839.
[44] V. Kuchtanin, L. Klescikova, M. Soral, R. Fischer, Z. Ruzickova, E. Rakovsky, J. Moncol, P. Segla, Polyhedron 117 (2016) 90–96.
[45] S. Layek, B. Agrahari, Anuradha, R. Ganguly, D.D. Pathak, J. Mol. Struct. 1141 (2017) 428–435.
[46] S. Priyarega, P. Kalaivani, R. Prabhakaran, T. Hashimoto, A. Endo, K. Natarajan, J. Mol. Struct. 1002 (2011) 58–62.
[47] I.K. Cıkla, S. Guveli, T.B. Demirci, M. Aygün, B. Ulkuseven, M. Yavuz, Polyhedron 130 (2017) 1–12.
[48] H.B. Shawish, M. Maah, S.N.A. Halim, S.A. Shaker, Arab. J. Chem. 9 (2016) 1935–1942.
[49] (a) R. Saswati, C.S. Dinda, E. Schmiesing, Y.P. Sinn, M. Patil, H.S. Nethaji, R. Evans, Acharyya, Polyhedron 50 (2013) 354–363;
(b) S. Saha, S. Jana, S. Gupta, A. Ghosh, H.P. Nayek, Polyhedron 107 (2016) 183–189.
[50] C.I. Someya, E. Irran, S. Enthaler, Inorg. Chim. Acta 421 (2014) 136–144.
[51] S. Guveli, S.A. Cınar, O. Karahan, V. Aviyente, B. Ulkuseven, 2016, Eur. J. Inorg. Chem. (2016) 538–544.
[52] (a) Zhengning Li, Zhuo Zheng, Boshun Wan, Huilin Chen, J. Mol. Catal. A Chem. 165 (2001) 67–71;
(b) M. Kim, T. Shin, A. Lee, H. Kim, Organometallics 37 (2018) 3253–3258.
[53] G.R. Bardajeea, M. Mohammadi, N. Kakavanda, Appl. Organomet. Chem. 30 (2016) 51–58.
[54] (a) M.N. Esfahani, I.M. Baltork, A.R. Khosropour, M. Moghadam, V. Mirkhani, S. Tangestaninejad, J. Mol. Catal. A Chem. 379 (2013) 243–254;
(b) L.Z. Fekri, M. Nikpassand, S. Shariati, B. Aghazadeh, R. Zarkeshvari, N. Norouz pour, J. Organomet. Chem. 871 (2018) 60–73.
[55] R. Karimian, S.J. Davarpanah, 2018, Appl. Organomet. Chem. (2018) 4529.
[56] V.G. Benítez, H. Valdes, S.H. Ortega, J.M.G. Acacio, D.M. Morales, Polyhedron 143 (2018) 144–148.
[57] SMART Version 5.628, Bruker AXS Inc., Madison, WI, USA, 2001.
[58] G.M. Sheldrick, SADABS, University of Gottingen, Gottingen, Germany, 1996.
[59] SHELXTL Version 5.1, Bruker AXS Inc., Madison, WI, USA, 1997.